Eur. Phys. J. Plus (2024) 139:936
https://doi.org/10.1140/epjp/s13360-024-05739-2

THE EUROPEAN PHYSICAL JOURNAL PLUS

Regular Article

Effects of magnetic, electric, and non-resonant intense laser fields on exciton binding energy and exciton absorption in a symmetric Gaussian single quantum well

Esin Kasapoglu[1,a], **M. B. Yücel**[2,b]

[1] Physics Department, Sivas Cumhuriyet University Science Faculty, 58140 Sivas, Türkiye
[2] Science Faculty, Physics Department, Akdeniz University, 07058 Antalya, Türkiye

Received: 5 August 2024 / Accepted: 10 October 2024
© The Author(s), under exclusive licence to Società Italiana di Fisica and Springer-Verlag GmbH Germany, part of Springer Nature 2024

Abstract The present study investigates the effects of external fields, including magnetic, electric, and non-resonant high-frequency intense laser fields, on the binding energies of the heavy hole excitons and the (hh1-e1) interband transitions from the ground state energy level of the heavy hole to the ground state energy level of the electron in GaAs/$Al_xGa_{1-x}As$ Gaussian type single quantum well. The study also considers the roles of the well width and the structure parameter. The results obtained show that the geometrical shape of the structure and the applied external fields are very effective tools on the excitonic binding and excitonic absorption spectra. From the results obtained, it was observed that the bandgap of semiconductor materials can be tuned by changing the structural parameters along with the applied external fields according to the purpose. This tunability enables the development of devices with optimized performance and new functionalities, thus driving innovation in various fields of technology.

1 Introduction

The quantum wells (QWs) can create a high carrier density in a small volume, this high density enhances the interaction with applied electric and magnetic fields, and the confined nature of the carriers means that even relatively small applied fields can have significant effects on their motion and energy states. The restrictions on the motion of the carriers confined in the low-dimensional semiconductor heterostructures of different sizes and shapes very clearly affect the linear and nonlinear optical properties of the materials, such as absorption, refractive index changes, second and third harmonic generation of these structures, and these properties are of great importance in the fabrication and applications of optoelectronic devices such as high-speed electro-optical modulators, optical switches, infrared photodetectors, semiconductor lasers, and far-infrared laser amplifiers [1–8]. QWs with smooth interfaces such as Gaussian-type QWs, as opposed to those with sharp interfaces, offer improved carrier confinement, reduced interface roughness, tailored electronic properties, and engineered nonlinear optical properties [9]. The Gaussian potential is smooth and differentiable, making it mathematically convenient for analytical and numerical calculations. This smoothness ensures that the potential energy does not have abrupt changes, which can be more realistic for certain physical systems. To fit the experimental data, Gaussian potentials which have different tuning parameters can be chosen. These parameters allow the potential to be fine-tuned according to the specific properties of the system under study. Empirical studies often show that Gaussian potentials can replicate the observed behavior of materials and molecules more accurately than other potential forms. This agreement with experimental data makes it a preferred choice in many applications [10]. Based on the Gaussian type potentials, a number of works have been reported to investigate the optical properties. Sari et al. studied the influence of position-dependent electron and heavy-hole mass distributions on the impurity-related electronic properties, excitonic binding energy, and intersubband electron transitions in a two-dimensional (2D) quantum dot with Gaussian potential [11]. Kasapoglu et al. considered the linear and nonlinear optical properties of an electron in both symmetrical and asymmetrical Gaussian type double quantum wells (DQWs) under an applied magnetic field [12], and non-resonant intense laser field (ILF) [13]. Guo and Du have reported their results for linear and nonlinear optical absorption coefficients and refractive index changes in asymmetrical Gaussian potential QW (AGCPQW) with an applied electric field [14]. Many theoretical researchers have reported asymmetric Gaussian confinement potential as an important factor in solving the polaron problem in QWs. For example, Dinh and Phuc investigated nonlinear phonon-assisted cyclotron resonance in AGCPQWs through a two-photon process [15]. Khordad et al. studied the temperature effect on bound polaron energy states and lifetime in AGCPQWs [16]. Sun and Xiao [17] explored the temperature effect on the magnetopolaron transition frequencies and state-energy levels in

[a] e-mail: ekasap@cumhuriyet.edu.tr (corresponding author)
[b] e-mail: myucel@akdeniz.edu.tr

Published online: 26 October 2024

asymmetric 2D Gaussian QWs. The application of exciton absorption in quantum wells is diverse, encompassing, but not limited to, photonics, optoelectronics, and quantum technologies. The capacity to alter excitonic characteristics through quantum confinement makes quantum wells an exceptionally versatile platform for developing next-generation devices. The coherent manipulation of excitons through exciton absorption is a crucial step in the development of quantum computing architectures. By tuning exciton absorption in quantum wells to interact with specific molecules, it is possible to create biosensing applications. Changes in excitonic properties, such as shifts in absorption spectra, can be used to detect biomolecules or chemical changes, which could lead to highly sensitive detectors for medical diagnostics or environmental monitoring. The study of excitons in low dimensional systems (LDSs) makes excitons easily tunable with a variety of external fields and different sample geometries, making them potential candidates for various applications in optics and optoelectronics [18]. Some of the research on excitons in LDSs is mentioned below. The effects of the transverse electric field on the electron and heavy hole energy levels, exciton binding energy and excitonic absorption spectra of GaAs parabolic quantum wires are theoretically investigated by S. Wu [19]. Acosta et al. investigated the exciton binding energy associated with the confined electron and hole states in cylindrical GaAs/GaAlAs quantum dots (QDs) [20]. Wang et al. investigated theoretically the pressure-dependent exciton binding energy and other optical properties such as interband emission energy and emission wavelength in a wurtzite (In,Ga)N-GaN coupled DQW structures under the built-in electric field [21]. The light-hole and heavy-hole exciton states and their optical properties, such as oscillator strength and radiative decay time, in asymmetric zinc-blende GaN/InGaN coupled DQWs are investigated in [22]. The combined effects of electric, magnetic, and intense terahertz laser fields on the exciton binding energy, interband transition energies (ITEs), dipole matrix elements, and absorption coefficients in a GaAs/AlGaAs semi parabolic QW are studied by A. John Peter et al. [23]. Yücel et al. investigated the ground-state binding energy and optical absorption coefficient of exciton in a symmetric double inverse parabolic quantum well system in the presence of external electric and magnetic fields [24], and Yücel et al. investigated the exciton binding energy and interband transitions between the electron and heavy-hole for the single and DQWs which have different hyperbolic type potential functions subject to electric, magnetic, and non-resonant intense laser fields [25]. To the best of our knowledge, excitons in symmetric Gaussian QWs have not been discussed so far. Therefore, this study aims to investigate the exciton binding energy and interband absorption in the symmetric GaAs/GaAlAs Gaussian single QW in the presence of the magnetic, electric and non-resonant ILF. The following is the organization of the paper: Sect. 2 presents the theoretical framework, while Sect. 3 is dedicated to the results and discussions. The conclusions are presented in Sect. 4.

2 Theory

In the effective mass approximation, the exciton Hamiltonian for the Gaussian type QW under the effects of the magnetic, electric and ILFs as follows

$$\hat{H} = \frac{1}{2m_{\mathrm{e}}^{*}}\left[\vec{p}_{\mathrm{e}} + \frac{e}{c}\vec{A}(\vec{r}_{\mathrm{e}})\right]^{2} + eFz_{\mathrm{e}} + V(z_{\mathrm{e}}, \alpha_o) + \frac{1}{2m_{\mathrm{h}}^{*}}\left[\vec{p}_{\mathrm{h}} - \frac{e}{c}\vec{A}(\vec{r}_{\mathrm{h}})\right]^{2} - eFz_{\mathrm{h}} + V(z_{\mathrm{h}}, \alpha_o) - \frac{e^{2}}{\varepsilon_o|\vec{r}_{\mathrm{e}} - \vec{r}_{\mathrm{h}}|} \tag{1}$$

where $m_{\mathrm{e}}^{*}(m_{\mathrm{h}}^{*})$ is the effective mass of the electron (heavy-hole), $\overrightarrow{p}_{\mathrm{e}}(\overrightarrow{p}_{\mathrm{h}})$ is the momentum of the electron (heavy-hole), $\overrightarrow{A}\left(\overrightarrow{r}\right)$ is the vector potential of the magnetic field, magnetic field is applied perpendicular to the growth direction (z-direction), i.e., the magnetic field and vector potential have the forms of $\overrightarrow{B} = (B, 0, 0)$ and $\overrightarrow{A} = (0, Bz, 0)$, e is the elementary charge, c is the speed of light, ε_o is the dielectric constant, F is the strength of the electric field which is applied parallel to the growth direction. In the absence of the ILF, the potential energy function in the modified form of the electron (hole) confined within Gaussian QW is given below [26]

$$V\left(z_{\mathrm{e(h)}}\right) = V_o^{\mathrm{e(h)}}\left(1 - e^{-q\left(\frac{z_{\mathrm{e(h)}}}{k}\right)^{2}}\right) \tag{2}$$

where $V_o^{\mathrm{e(h)}}$ is the band discontinuity for electron (hole), $V_o^{\mathrm{e}} = 228\mathrm{me}V$ and $V_o^{\mathrm{h}} = 176\mathrm{me}V$, these values are for aluminum concentration value of $x = 0.3$ in $\mathrm{GaAs/Al}_x\mathrm{Ga}_{1-x}\mathrm{As}$ QWs. In Eq. (2), q-parameter is a dimensionless parameter that controls the well width. The parameter-k is the well width, and it defines also the effective range of the Gaussian QW.

In the presence of the non-resonant ILF, the potential energy function-$V\left(z_{\mathrm{e(h)}}, \alpha_0\right)$ which is called laser-dressed potential is as given in Eq. (3) [12]

$$V\left(z_{\mathrm{e(h)}}, \alpha_0\right) = \frac{\omega_0}{2\pi}\int_0^{\frac{2\pi}{\omega_0}} V\left(z_{\mathrm{e(h)}} + \alpha_0 \sin(\omega_0 t)\right)\mathrm{d}t \tag{3}$$

where $\alpha_o = eA_o/m^{*}\omega_o$, A_0 and ω_o are the laser-dressed or ILF parameter, the magnitude of the vector potential and the angular frequency of the non-resonant ILF, respectively. The details of the equations given above for dressed potentials and the non-

perturbative approach based on the Kramers-Henneberger translation transformation developed to describe the atomic behavior in intense high-frequency ILF can be found in Refs. [27].

By defining the electron–hole center of mass ($\overrightarrow{R} = m_e^* \overrightarrow{r}_e + m_h^* \overrightarrow{r}_h / m_e^* + m_h^*$) and the relative coordinate ($\overrightarrow{r} = \overrightarrow{r}_e - \overrightarrow{r}_h$), and assuming that the motion of the center of mass is constant, the exciton Hamiltonian in cylindrical coordinates is obtained as follows

$$\widehat{H} = -\frac{\hbar^2}{2\mu}\left(\frac{\partial^2}{\partial\rho^2} + \frac{1}{\rho}\frac{\partial}{\partial\rho} + \frac{1}{\rho^2}\frac{\partial^2}{\partial\varnothing^2}\right) - \frac{\hbar^2}{2m_e^*}\frac{\partial^2}{\partial {z_e}^2} - \frac{\hbar^2}{2m_h^*}\frac{\partial^2}{\partial {z_h}^2} - \frac{eB}{c}\left(\frac{z_e}{m_e^*} + \frac{z_h}{m_h^*}\right)p_y + \frac{e^2B^2\hbar^2}{4\mu m_e^* c^2 R_y^2}z_e^2 + \frac{e^2B^2\hbar^2}{4\mu m_h^* c^2 R_y^2}z_h^2 - \frac{e^2}{\varepsilon_o\sqrt{\rho^2 + (z_e - z_h)^2}} + V(z_e, \alpha_o) + eFz_e + V(z_h, \alpha_o) - eFz_h \tag{4}$$

where $\rho(= [(x_e - x_h)^2 + (y_e - y_h)^2]^{\frac{1}{2}})$ is the relative distance between the electron and hole in the *(x–y)* plane, $\mu(= m_e^* m_h^* / (m_e^* + m_h^*))$ is the reduced mass, $\mathrm{Ry}(= \mu e^4 / 2\varepsilon_o^2\hbar^2)$ is the exciton Rydberg. It should be noted that the 4th term in Eq. (4) equals to zero ($[z,\ p_y] = 0$). By scaling the lengths and energies with respect to the exciton Bohr radius ($a_B = \varepsilon_o^2\hbar^2/\mu e^2$) and the exciton Rydberg, the dimensionless Hamiltonian for the exciton is written as follows

$$\tilde{H} = -\left(\frac{1}{\rho}\frac{\partial}{\partial\rho} + \frac{\partial^2}{\partial\rho^2} + \frac{1}{\rho^2}\frac{\partial^2}{\partial\emptyset^2}\right) - \frac{\mu}{m_e^*}\frac{\partial^2}{\partial z_e^2} + V(z_e, \alpha_o) + Fz_e - \frac{\mu}{m_h^*}\frac{\partial^2}{\partial z_h^2} + V(z_h, \alpha_o) - Fz_h + \frac{e^2B^2\hbar^2}{4\mu m_e^* c^2 R_y^2}z_e^2 + \frac{e^2B^2\hbar^2}{4\mu m_h^* c^2 R_y^2}z_h^2 - \frac{2}{\sqrt{\rho^2 + (z_e - z_h)^2}} \tag{5}$$

For the excitonic structure, by choosing the wavefunction in the form of

$$\Phi(\widetilde{\rho}, \phi, \widetilde{z}_e, \widetilde{z}_h, \lambda) = \psi(\widetilde{z}_e)\psi(\widetilde{z}_h)\varphi(\widetilde{\rho}, \lambda) \tag{6}$$

Schrödinger equation $\widetilde{H}(\widetilde{\rho},\ \phi,\ \widetilde{z}_e,\ \widetilde{z}_h)\Phi(\widetilde{\rho},\ \phi,\ \widetilde{z}_e,\ \widetilde{z}_h,\ \lambda) = \widetilde{E}\Phi(\widetilde{\rho},\ \phi,\ \widetilde{z}_e,\ \widetilde{z}_h,\ \lambda)$ for the Hamiltonian in Eq. (5) is solved. Here E, $\psi(z_e)$ and $\psi(z_h)$ are the total energy, the wavefunctions of the electron and hole in the z-direction, respectively. The wave function with λ variational parameter describing the exciton motion in the xy plane is given by [28–30]

$$\varphi(\rho, \lambda) = \frac{1}{\lambda}\sqrt{\frac{2}{\pi}}e^{-\frac{\rho}{\lambda}} \tag{7}$$

At the same time the variational parameter- λ means the increase in the exciton wave function extension. E_{1e} and E_{1hh} are the ground state energies of the electron and heavy hole, respectively. After the subband energies and the expectation value of the Hamiltonian in Eq. (5) are obtained, the exciton binding energy (E_b) is defined as follows

$$E_b = E_{1e} + E_{1hh} - {}^{\min}_{\lambda}\langle\Phi|H|\Phi\rangle. \tag{8}$$

It should be noted that the value of λ which minimizes the energy is determined numerically.

In the dipole approximation, the general expression for the linear absorption coefficient corresponding to the excitonic transition for the heavy hole-electron is given by [25, 28, 31]

$$\alpha(\omega) = \frac{1}{V}\frac{4\pi^2e^2}{\mathrm{nc}m_o^2\omega}\sum_{i,f}|\langle i|\widehat{\varepsilon}\widehat{p}|f\rangle|^2\delta(E_f - E_i - \hbar\omega), \tag{9}$$

where ω is the angular frequency of the incident photon, $V(= k_x k_y k_z)$ is the volume of the sample, n is the refractive index refraction of the material, $\widehat{\varepsilon}$ is the polarization vector of the incident radiation, $\widehat{p}$ is the momentum operator of electron, $\langle i| = \langle\psi_{1hh}(z_h)|$ and $|f\rangle = |\psi_{1e}(z_e)\rangle$ are initial and final states of system, respectively.

$$|\langle i|\widehat{\varepsilon}\widehat{p}|f\rangle|^2 = |\langle U_V|\widehat{\varepsilon}\widehat{p}|U_C\rangle|^2\left|\langle\psi_i(z_h)|\psi_f(z_e)\rangle\right|^2\delta_{\boldsymbol{K}_\perp,0}k_x k_y|g_t(\rho = 0, \lambda|^2 \tag{10}$$

where k_x and k_y are the lengths in free dimensions, and $\boldsymbol{K}_\perp = \boldsymbol{k}_{\perp C} - \boldsymbol{k}_{\perp V}$ is the difference between the conduction and valance band electron wave vectors. δ function dictates that, for the interband transitions, the electron momentum in the x and y directions is conserved. $g_t(\rho = 0,\ \lambda)$ term indicates that only excitons with an amplitude different from zero can absorb light at $\rho = 0$. The allowed optical transitions between the first heavy hole and the first electron subbands are given by

$$|\langle U_V|p_z|U_C\rangle|^2 = \frac{m_o}{4}E_p \tag{11}$$

Here, E_p is the Kane matrix element. So, for the excitons in a 2D QWs the absorption coefficient in Eq. (9) for heavy hole-electron transition (hh1-e1) reduces to

$$\alpha(\omega) = \frac{1}{k_{\mathrm{eff}}\lambda^2}\frac{e^2E_p}{\mathrm{nc}m_0\omega}|\langle\psi_i(z_h)|\psi_f(z_e)\rangle|^2\frac{\Gamma}{\left(E_{1e} + E_{1hh} + E_g^{\mathrm{GaAs}} - E_b - \hbar\omega\right)^2 + (\Gamma/2)^2} \tag{12}$$

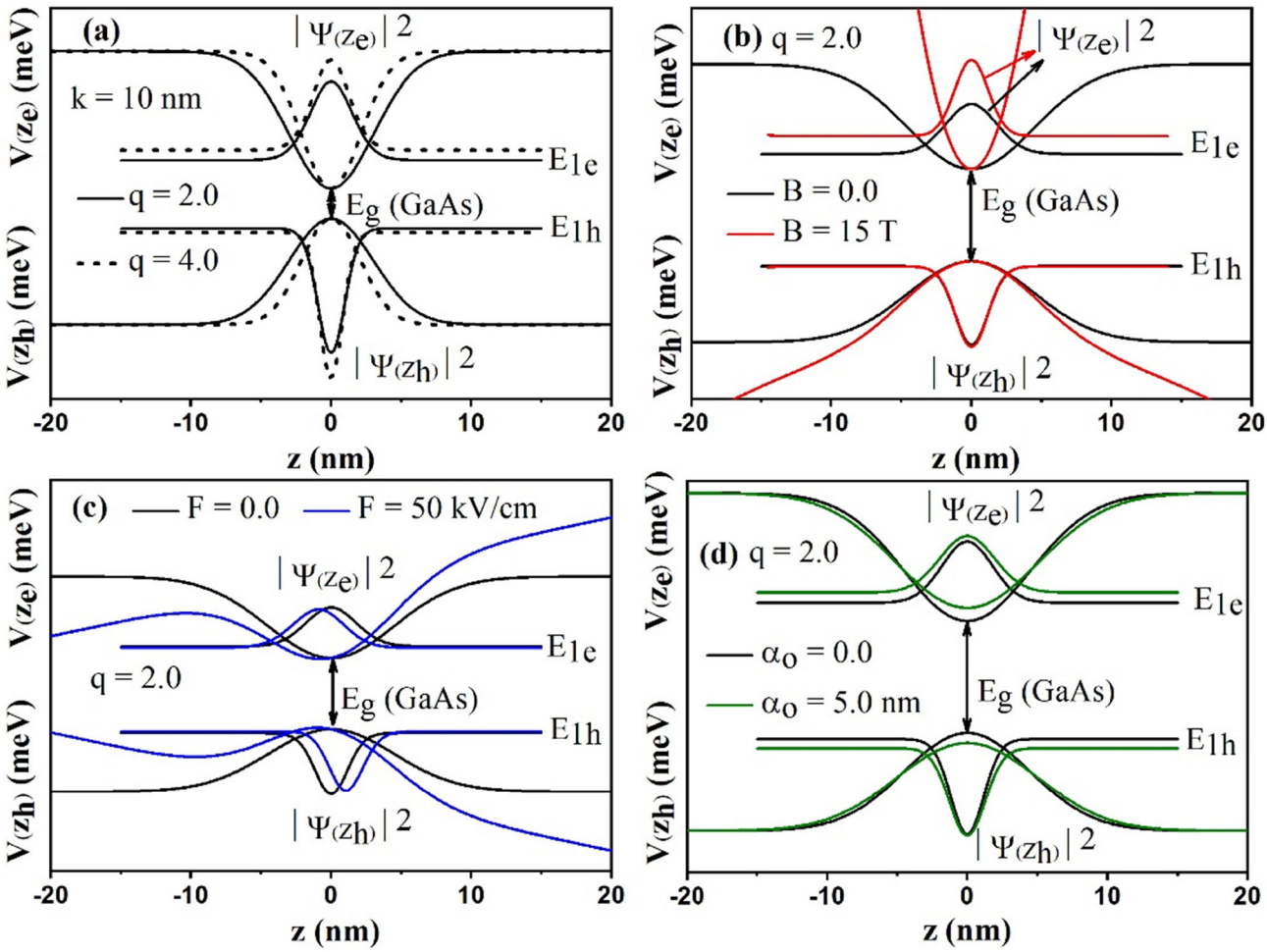


Fig. 1 The confinement potentials and the ground state squared wave functions of the electron and the hole in a Gaussian quantum well versus the z-coordinate for two different q-values and $k = 10nm$: in the absence of any external field (**a**), in the absence and presence of the magnetic field (**b**), in the absence and presence of the electric field (**c**), and in the absence and presence of the non-resonant intense laser field (**d**). The energy axis value of the wave functions shows the energy of the relevant level

where $k_{\text{eff}}(= k)$ is the effective well width, $I_o = \langle\psi_{\text{i}}(z_{\text{h}})|\psi_{\text{f}}(z_{\text{e}})\rangle$ is the overlap integral between the electron and heavy-hole, Γ is the broadening parameter, $E_{\text{g}}^{\text{GaAs}}$ is the band gap of GaAs and $\hbar\omega$ is photon energy required for the transition to conduction band from valance band, and finally the term $(E_{1\text{e}} + E_{1\text{hh}} + E_{\text{g}}^{\text{GaAs}} - E_{\text{b}})$ in the denominator of the last factor in Eq. (12) is the ITE, where $E_{1\text{e}} + E_{1\text{hh}} + E_{\text{g}}^{\text{GaAs}}$ is the band gap of the system [32].

3 Results and Discussion

The values of our parameters are $m_{\text{e}}^* = 0.067m_o, m_{\text{h}}^* = 0.45m_o, \mu = 0.04m_o, m_o$ is the free electron mass, $\varepsilon_o = 12.58, \Gamma = 1$ meV, $E_{\text{p}} = 25.7$eV, $E_{\text{g}}^{\text{GaAs}} = 1.424eV$ [25, 28].

In the absence and presence of the external field, the Gaussian QW potentials which are confined the electron in the conduction band and the hole in the valence band and the variations of the square wave functions corresponding to the ground state energies of these particles versus the z coordinate for $k = 10$nm are shown in Fig. 1. The values of applied external fields and structure parameters are indicated in the figures to which it belongs. Figure 1a is given for two different q-values and without any external field. The increase in the q-parameter causes an increase in well width. The magnetic field creates an additional parabolic constraint on the Gaussian QW. As seen in Fig. 1b, the magnetic field effect for the electron is quite pronounced, for the electron the magnetic field causes the Gaussian QW with finite barrier to transform into infinite parabolic QW, the potential barrier for the hole is just beginning to rise toward infinity, since the effective mass of the hole is much heavier than the electron. It can be seen in Fig. 1 c that an external electric field applied along the growth direction (z direction) causes the Gaussian QWs confining the electron and

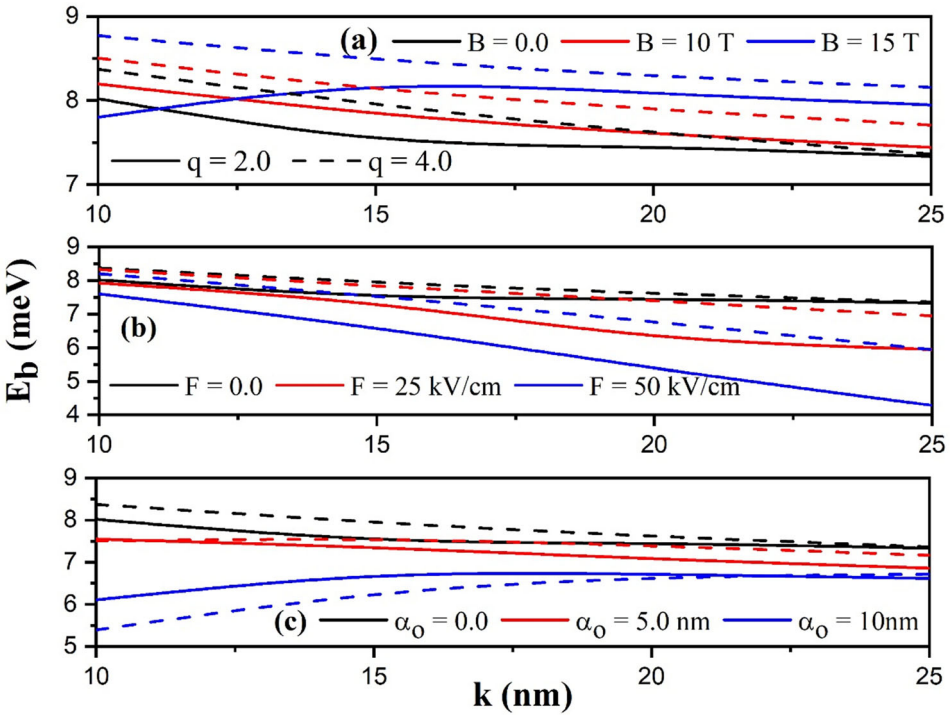


Fig. 2 a-c The variations of the binding energies of heavy hole excitons in the Gaussian QW as a function of the well width-k under the magnetic, electric, and intense laser fields, respectively. The solid (dashed) lines are for $q = 2.0$ ($q = 4.0$). The values of applied external fields and structure parameters are indicated in the figures to which it belongs

the hole to bend in opposite directions. Figure 1d shows that ILF causes the minimum point of the well potential to shift to higher energies. Note that the details of the effects of ILF on the Gaussian QW structure will be given in the corresponding figures.

Figure 2a–c shows the variation of the binding energies of heavy hole excitons in the Gaussian QW as a function of the well width-k under the magnetic, electric, and intense laser fields, respectively. The solid (dashed) lines are for $q = 2.0$ ($q = 4.0$). The changes in the heavy hole exciton binding energies under the effects of k and q parameters as well as each applied external field are as follows: (i) In general, as the well width increases, the exciton binding energy (E_b) decreases, since the overlap integral (I_o) between the electron and the hole wave functions increases, except in special cases in the range of $10nm \leq k \leq 15nm$ depending on the some values of the magnetic field and ILF, and structural parameters (see the solid blue line in Fig. 2 (a), and the both solid and dashed blue lines in Fig. 2c). (ii) As seen in Fig. 1a, since the q-parameter causes a narrowing of the well width, I_o decreases, therefore an increase in the exciton binding energy is observed as q increases. (iii) The magnetic field creates an additional parabolic confinement on the Gaussian QW, therefore, the presence of the magnetic field leads to more binding due to more confinement, except for special cases. As the magnetic field increases, the Gaussian QW potential in which the electron is confined turns into an infinite parabolic QW. Furthermore, the magnetic field also causes the squeezing of the carrier wave functions. While the structure change caused by the magnetic field is observed for the electron, it is not yet observed for the hole in the same conditions, only the barrier height just starts to increase toward infinity (see Fig. 1b). Undoubtedly, this is the fact that the effective mass of the hole is much heavier than that of the electron. It should also be noted that while the magnetic field causes a significant increase in the energy of the electron, almost no change in the energy of the hole is observed. Because, the electron wave function becomes more and more confined around the center of the structure, whereas the hole wave function remains almost unaffected. These changes for the Gaussian QW potential surrounding the hole will occur at larger magnetic field values or at larger well widths (for example$k = 15$nm). Therefore, for $q = 2.0$ and$B = 15T$, E_b increases up to a certain k-value and starts to decrease after the value of$k \geq 15nm$. Because the hole is now fully affected by the magnetic field confinement just like the electron due to the weakening of the geometric confinement. (iv) An external electric field applied along the growth direction (z-direction) causes the Gaussian QWs confining the electron and hole to bend in opposite directions. Since the electric field pushes the electron toward the left side and the hole toward the right side of the QWs, the overlap of the wave functions of the electron–hole pair and therefore the Coulomb interaction between them also decreases. As a result, the exciton binding energy decreases with the effect of the electric field. As increasing k-value weakens the geometric confinement, the electric field effect becomes more pronounced. Therefore, as increasing q-value causes stronger confinement, for $q = 4.0$, E_b is less sensitive to the electric field than that of $q = 2.0$. (v) The minimum of the Gaussian QW shifts to higher energies, while the barrier height decreases. Therefore, in the presence of ILF, the probability of seeing each other in the same plane decreases due to the increase in the energy of the particles, and the overlap integral (I_o) and the exciton wave function extension (λ) also increase. All these reasons cause a decrease in the E_b. In the presence of ILF, for sufficiently large laser dressed parameters (α_o) as the well width-k increases, the energies of the particles and the exciton wave function extension decrease, thus E_b increases up to a certain k-value and then it decreases with increasing k-value. For $q = 2.0$, E_b is larger than at $q = 4.0$, but this

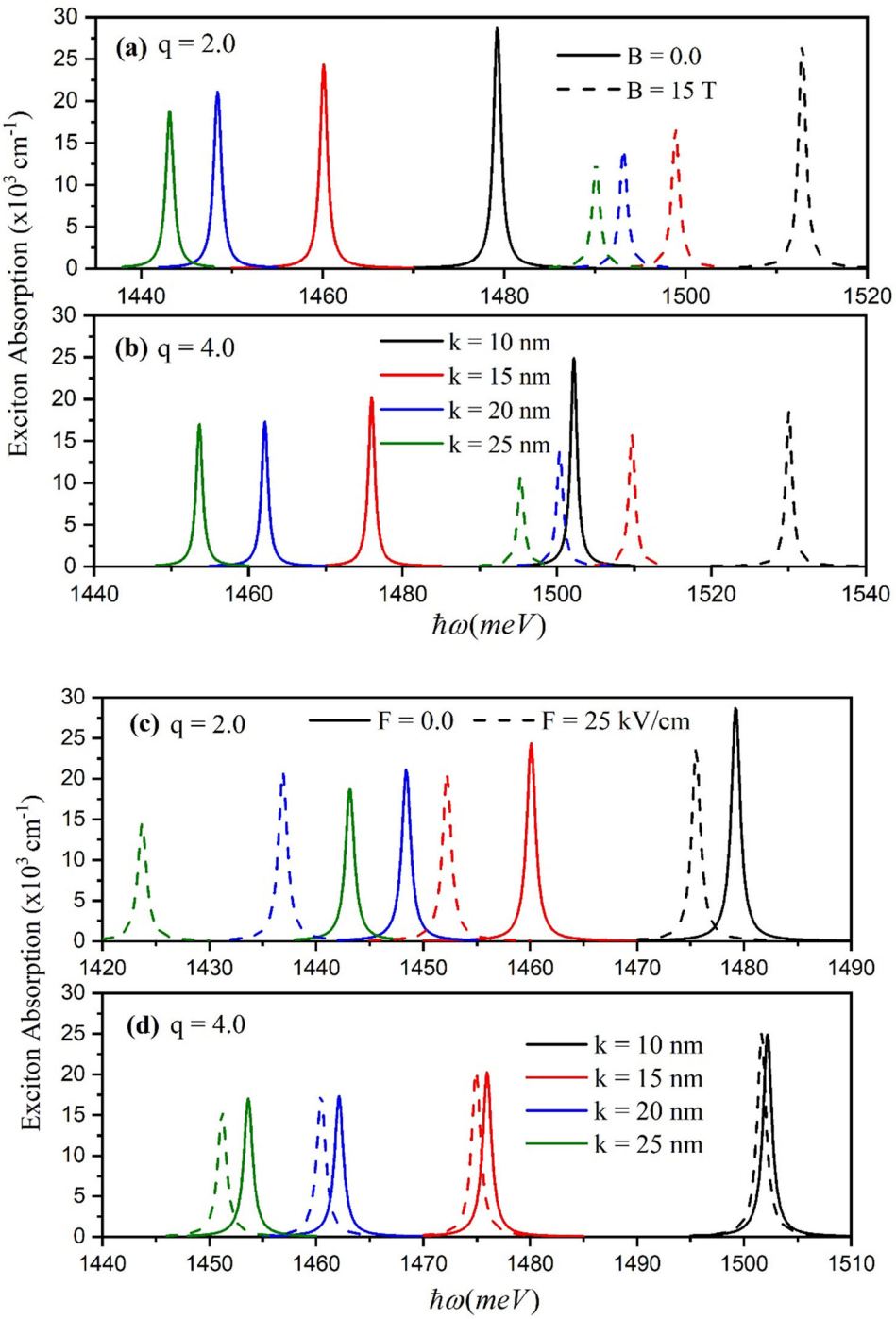
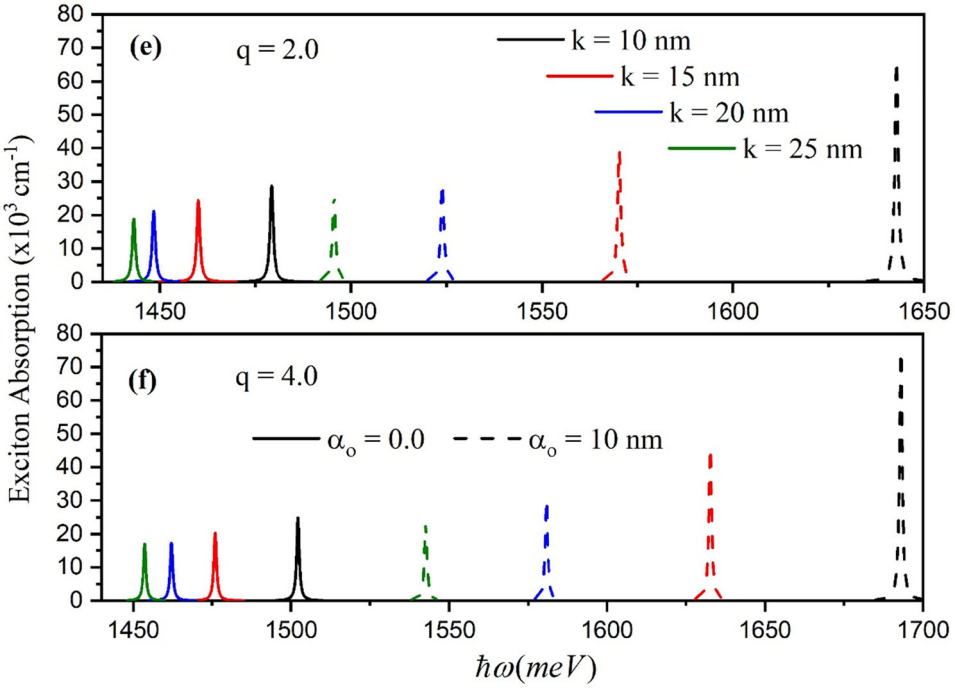


Fig. 3 The exciton absorption coefficients for the (hh1-e1) interband transitions in Gaussian QW as a function of the resonant photon energy for different well widths: in the absence and presence of the magnetic field (**a**,**b**), in the absence and presence of the electric field (**c**,**d**), and in the absence and presence of the non-resonant intense laser field (e, f), respectively. Each applied external field is indicated in the figures to which it belongs. The results of Figs. 3 (**a**), (**c**) and (**e**) are for $q = 2.0$, and the rest is for $q = 4.0$

behavior reverses from $k \geq 20nm$ due to the variation in the λ-value. It should also be noted that the structure can be transformed from a single QW to a double QW by changing the structure parameters such as the k and q-parameters together with the ILF effect. For example, for $\alpha_o = 10nm$ and$k = 10nm$, the structure is a single QW at $q = 2.0$, while it is a double QW at $q = 4.0$.

The exciton absorption coefficients (EACs) for the (hh1-e1) interband transitions in Gaussian QW as a function of the resonant photon energy for different well widths and applied external fields such as the magnetic field, the electric field, and the non-resonant intense laser field are given in Figs. 3a–e for $q = 2.0$ and Figs. 3b–f for $q = 4.0$. The (hh1-e1) represents the transition from the ground state energy level of the heavy hole in the valence band to the ground state energy level of the electron in the conduction band. Please also consider Figs. 4, 5 and 6. Figures 4a–c, 5a–c, 6a–c are given to show how the ITE, the overlap integral, and the exciton wave function extension, which are the effective parameters for the changes in the positions and amplitudes of the exciton absorption peaks and on the exciton binding energy, change as a function of the structure parameters and all applied external fields.

Fig. 3 continued



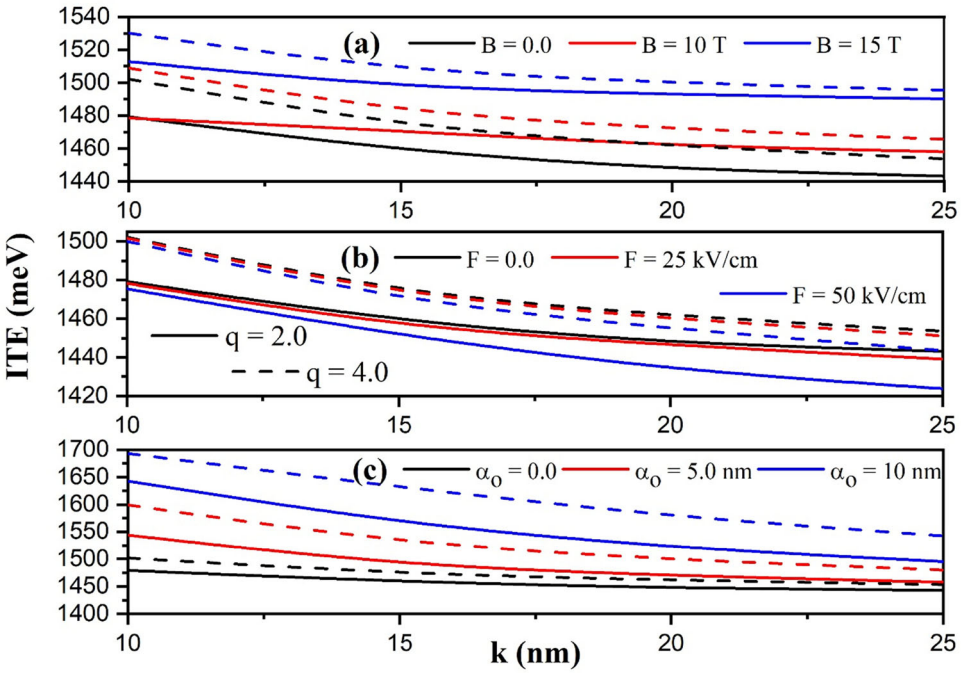


Fig. 4 **a-c** The interband transition energies ($= E_{1e} + E_{1h} + E_g^{GaAs} - E_b$) versus the k-parameter for $q = 2.0$ (solid lines) and $q = 4.0$ (dashed lines): with and without magnetic field (**a**), with and without electric field (**b**), and with and without non-resonant intense laser field (**c**), respectively

The changes in the positions and amplitudes of the EACs as a function of the structure parameters and the applied external fields are as follows. (i) As the k-well width increases, the positions of the EACs shift toward the lower photon energies with decreasing amplitudes due to the decrease in the ITE ($= E_{1e} + E_{1h} + E_g^{GaAs} - E_b$). The ITE decreases due to the decrement of the electron and hole energies with increasing well size, and the amplitudes of the EACs decrease due to the increase of the spatial spread of the electron and hole wave functions, the exciton wave function extension (λ), and the overlap integral (I_o) between the electron and hole wave functions. (ii) Since the increase of the q-parameter creates a strong confinement for both the electron and hole, the positions of the EACs shift toward higher photon energies due to the increase of the ITE, as can be seen in all subplots of Fig. 3. (iii) The magnetic field causes an increase in the ITE due to the increase in electron and hole energies, so the EACs shift to the higher photon energies. The magnetic field causes a decrease in the overlap integral, which is mainly related to the squeezing of the carrier wave functions around the well center, which is the reason for the decrease in the amplitude of the EACs. (iv) Since the ITE

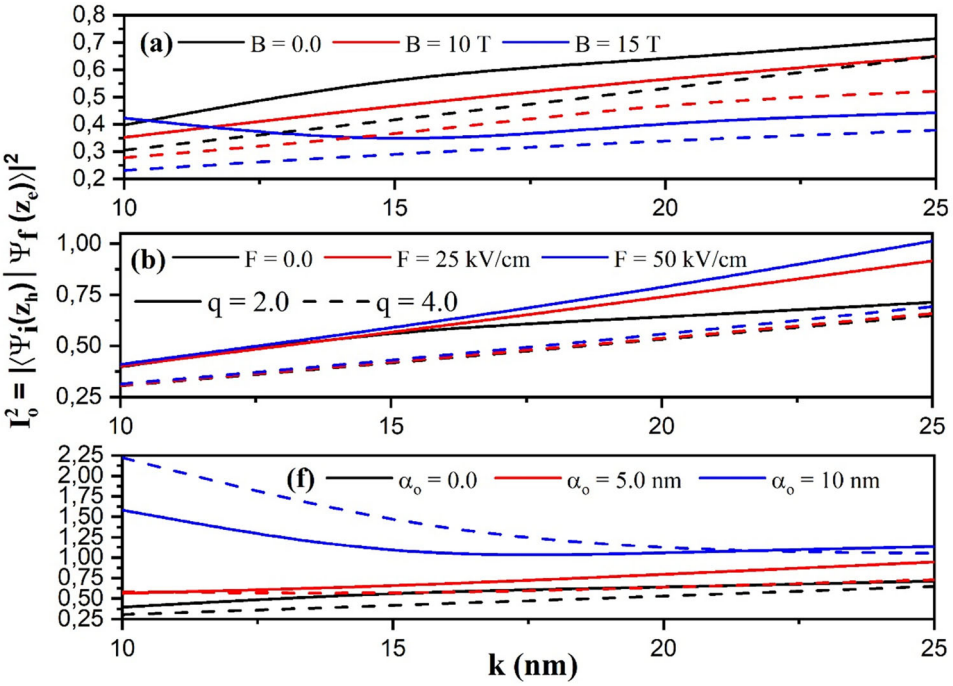


Fig. 5 **a-c** The squared overlap integral versus the k-parameter for $q = 2.0$ (solid lines) and $q = 4.0$ (dashed lines): with and without magnetic field (**a**), with and without electric field (**b**), and with and without non-resonant intense laser field (**c**), respectively

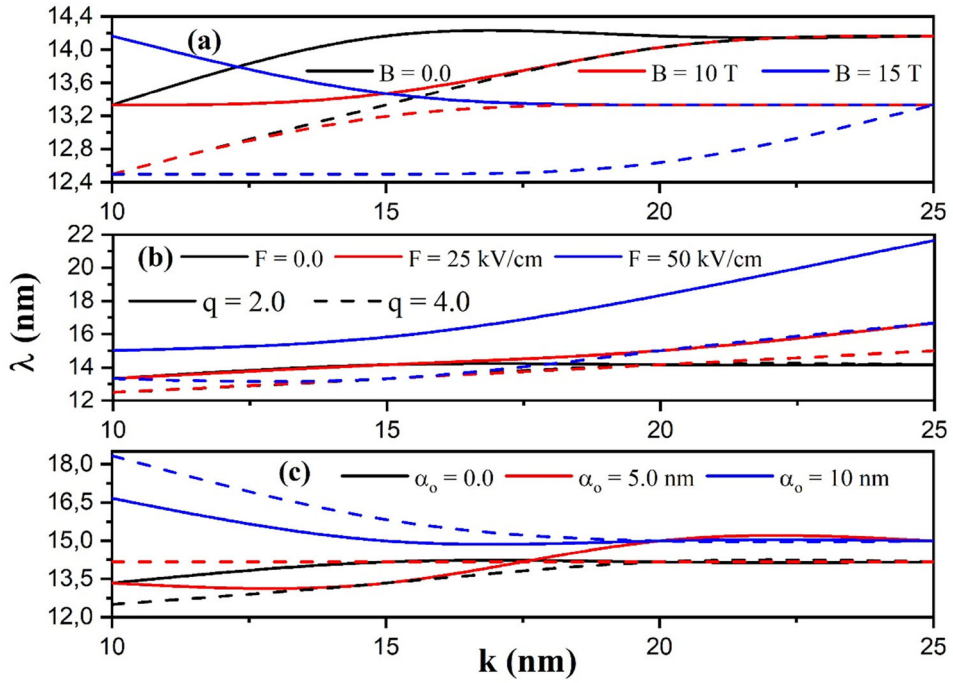


Fig. 6 **a-c** The exciton extension versus the k-parameter for $q = 2.0$(solid lines) and $q = 4.0$ (dashed lines): with and without magnetic field (**a**), with and without electric field (**b**), and with and without non-resonant intense laser field (**c**), respectively

is reduced with the effect of the electric field, the EACs are shifted to lower photon energies, and since there is also an increase in the exciton extension despite the increase in the overlap integral, a decrease in the amplitude of the peaks is observed, but not as much as in the magnetic field. (v) With the effect of ILF, the exciton absorption peak positions shift to the higher photon energies with increasing amplitudes.

4 Conclusion

In this work, we have investigated the effects of structure parameters and applied external fields, such as the magnetic, electric, and non-resonant high-frequency intense laser fields, on the exciton binding energy and interband absorption including the (hh1-e1)

transitions in a symmetric GaAs/GaAlAs Gaussian single quantum well. The results obtained show that the geometrical shape of the structure and the applied external fields are very effective tools on the exciton binding energy and exciton absorption spectra. As a result, the exciton binding energy and interband transitions are critical to the functionality and optimization of a wide range of technologies in optoelectronics and photonics. The freedom to tune the bandgap of the material of interest by applied external fields, structural geometry, and structural parameters allows the design of materials that absorb or emit light at specific wavelengths. This is particularly useful for optoelectronic devices such as LEDs and lasers.

Data Availability The manuscript has associated data in a data repository. [Author's comment: Data will be made available on request.]

References

1. N.D. Hien, Linear and nonlinear optical properties in quantum wells. Micro and Nanostruct. **170**, 207372 (2022). https://doi.org/10.1016/j.micrna.2022.207372
2. N.D. Hien, Optical properties of a single quantum well with Pöschl-Teller confinement potential. Physica E **145**, 115504 (2023). https://doi.org/10.1016/j.physe.2022.115504
3. N.D. Hien, Comparison of the nonlinear optical properties of asymmetrical and symmetrical quantum wells. Eur. Phys. J. B. **95**, 192 (2022). https://doi.org/10.1140/epjb/s10051-022-00455-1
4. J. You, K. Guo, J. Lao, S. Mo, Linear and nonlinear optical absorption coefficients and refractive index changes of zigzag quantum wells affected by terahertz laser field. Thin Solid Films **733**, 138813 (2021). https://doi.org/10.1016/j.tsf.2021.138813
5. L. Zhang, H.J. Xie, Electric field effect on the second-order nonlinear optical properties of parabolic and semiparabolic quantum wells. Phys. Rev. B **68**, 235315 (2003). https://doi.org/10.1103/PhysRevB.68.235315
6. G. Wang, Third-harmonic generation in cylindrical parabolic quantum wires with an applied electric field. Phys. Rev. B **72**, 155329 (2005). https://doi.org/10.1103/PhysRevB.72.155329
7. L. Zhang, J.J. Shi, Calculation of linear and nonlinear intersubband refractive-index changes in an asymmetrical semiparabolic quantum well with applied electric field. Phys. Stat. Sol. (b) **242**, 1001 (2005). https://doi.org/10.1002/pssb.200402130
8. H. Yıldırım, M. Tomak, Nonlinear optical properties of a Pöschl-Teller quantum well. Phys. Rev. B **72**, 115340 (2005). https://doi.org/10.1103/PhysRevB.72.115340
9. M. Yoshita, H. Akiyama, L.N. Pfeiffer, K.W. West, Quantum wells with atomically smooth interfaces. Appl. Phys. Lett. **81**, 49–51 (2002). https://doi.org/10.1063/1.1490144
10. S. Klawohn, J.P. Darby, J.R. Kermode, G. Csányi, M.A. Caro, A.P. Bartók, Gaussian approximation potentials: theory, software implementation and application examples. J. Chem. Phys. **159**, 174108 (2023). https://doi.org/10.1063/5.0160898
11. H. Sari, E. Kasapoglu, S. Sakiroglu, I. Sökmen, C.A. Duque, Effect of position-dependent effective mass on donor impurity- and exciton-related electronic and optical properties of 2D gaussian quantum dots. Eur. Phys. J. Plus **137**, 341 (2022). https://doi.org/10.1140/epjp/s13360-022-02491-3
12. E. Kasapoglu, M.B. Yücel, C.A. Duque, Parabolic-gaussian double quantum wells under a nonresonant intense laser field. Nanomaterials **13**(8), 1360 (2023). https://doi.org/10.3390/nano13081360
13. E. Kasapoglu, M.B. Yücel, C.A. Duque, Harmonic-gaussian symmetric and asymmetric double quantum wells: magnetic field effects. Nanomaterials **13**, 892 (2023). https://doi.org/10.3390/nano13050892
14. A.X. Guo, J.F. Du, Linear and nonlinear optical absorption coefficients and refractive index changes in asymmetrical Gaussian potential quantum wells with applied electric field. Superlatt. Microstruct. **64**, 158–166 (2013). https://doi.org/10.1016/j.spmi.2013.08.030
15. L. Dinh, H.V. Phuc, Nonlinear phonon-assisted cyclotron resonance via two-photon process in asymmetrical Gaussian potential quantum wells. Superlattice. Microst. **86**, 111 (2015). https://doi.org/10.1016/j.spmi.2015.07.034
16. R. Khordad, S. Goudarzi, H. Bahramiyan, Effect of temperature on lifetime and energy states of bound polaron in asymmetrical Gaussian quantum well. Indian J. Phys. **90**, 659 (2016). https://doi.org/10.1007/s12648-015-0790-9
17. Y. Sun, J.-L. Xiao, Temperature effects on state-energy levels and transition frequency of magnetopolaron in asymmetric two-dimensional Gaussian quantum wells. J. Nanophotonics **12**, 046004 (2018). https://doi.org/10.1117/1.JNP.12.046004
18. M.C. Beard, R.J. Ellingson, Multiple exciton generation in semiconductor nanocrystals: Toward efficient solar energy conversion. Laser Photon. Rev. **2**, 377–399 (2008). https://doi.org/10.1002/lpor.200810013
19. S. Wu, Exciton binding energy and excitonic absorption spectra in a parabolic quantum wire under transverse electric field. Phys. B **406**, 4634–4638 (2011). https://doi.org/10.1016/j.physb.2011.09.047
20. R.E. Acosta, A. Zapata, C.A. Duque, M.E., Mora-Ramos, Electric field effects on excitons in cylindrical quantum dots with asymmetric axial potential. Influ. nonlinear opt. prop. Phys. E **44**, 1936–1944 (2012). https://doi.org/10.1016/j.physe.2012.05.027
21. G.X. Wang, X.Z. Duan, Built-in electric field and hydrostatic pressure effects on exciton states in a wurtzite (In, Ga)N/GaN coupled double quantum well. J. Korean Phys. Soc. **83**, 426–436 (2023). https://doi.org/10.1007/s40042-023-00876-w
22. G.X. Wang, X.N. Li, X.Z. Duan, Effects of strain and hydrostatic pressure on exciton properties in asymmetric zinc-blende (In, Ga)N/GaN coupled double quantum wells. J. Phys. Chem. Solids **173**, 111107 (2023). https://doi.org/10.1016/j.jpcs.2022.111107
23. A. John Peter, E. Kasapoglu, M.E. Mora-Ramos, F. Ungan, Effects of external perturbations on light absorption by light/ heavy hole excitons in a semi-parabolic quantum well. J. Mol. Struct. (2023). https://doi.org/10.1016/j.molstruc.2022.134438
24. M.B. Yücel, S. Sakiroglu, H. Sari, C.A. Duque, E. Kasapoglu, Influence of external fields on the exciton binding energy and interband absorption in a double inverse parabolic quantum well. Physica E **144**, 115433 (2022). https://doi.org/10.1016/j.physe.2022.115433
25. M.B. Yücel, H. Sari, C.M. Duque, C.A. Duque, E. Kasapoglu, Theoretical study of the exciton binding energy and exciton absorption in different hyperbolic-type quantumwells under applied electric, magnetic, and intense laser fields. Int. J. Mol. Sci. **23**, 11429 (2022). https://doi.org/10.3390/ijms231911429
26. H. Sari, S. Sakiroglu, Molecular complex states and intersubband transitions in a quantum ring under gaussian repulsive potential. Eur. Phys. J. Plus **139**, 244 (2024). https://doi.org/10.1140/epjp/s13360-024-05064-8
27. M. Panda, T. Das, B.K. Panda, Nonlinear optical properties in the laser-dressed two-level $Al_xGa_{1-x}N$/GaN single quantum well. Int. J. Mod. Phys. B **31**, 1850032 (2017). https://doi.org/10.1142/S0217979218500327
28. E. Kasapoglu, I. Sökmen, I., Interband absorption and exciton binding energy in an inverse parabolic quantum well under the magnetic field. Phys. Letters A (2007). https://doi.org/10.1016/j.physleta.2007.06.072

29. G. Bastard, Hydrogenic impurity states in a quantum well: A simple model. Phys. Rev. B **24**, 4714 (1981). https://doi.org/10.1103/PhysRevB.24.4714
30. A. Latge, N. Porras-Montenegro, M. De Dios-Leyva, L.E. Oliveira, Intradonor absorption spectra under external fields in quantum wells. Phys. Rev. B **53**, 10160 (1996). https://doi.org/10.1103/PhysRevB.53.10160
31. F. Bassani, G. Pastori Parravicini, *Electronic States and Optical Transitions in Solids* (Pergamon, New York. p, 1975), p.152
32. G. Bastard, *Wave Mechanics Applied to Semiconductor Heterostructures* (United States, Halsted, 1988), p.1990

Springer Nature or its licensor (e.g. a society or other partner) holds exclusive rights to this article under a publishing agreement with the author(s) or other rightsholder(s); author self-archiving of the accepted manuscript version of this article is solely governed by the terms of such publishing agreement and applicable law.